

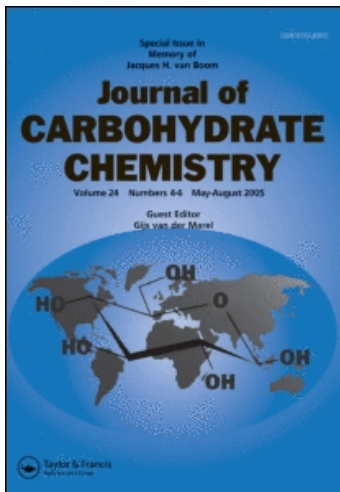
This article was downloaded by:

On: 23 January 2011

Access details: *Access Details: Free Access*

Publisher *Taylor & Francis*

Informa Ltd Registered in England and Wales Registered Number: 1072954 Registered office: Mortimer House, 37-41 Mortimer Street, London W1T 3JH, UK



## Journal of Carbohydrate Chemistry

Publication details, including instructions for authors and subscription information:

<http://www.informaworld.com/smpp/title~content=t713617200>

### Molecular Mechanics Modeling of $\alpha$ -(1 $\rightarrow$ 2)-, $\alpha$ -(1 $\rightarrow$ 3)-, and $\alpha$ -(1 $\rightarrow$ 6)-Linked Mannosyl Disaccharides with MM3(92)<sup>1</sup>

Michael K. Dowd<sup>a</sup>; Alfred D. French<sup>a</sup>; Peter J. Reilly<sup>b</sup>

<sup>a</sup> U. S. Department of Agriculture, Southern Regional Research Center, New Orleans, LA <sup>b</sup> Department of Chemical Engineering, Iowa State University, Ames, IA

**To cite this Article** Dowd, Michael K. , French, Alfred D. and Reilly, Peter J.(1995) 'Molecular Mechanics Modeling of  $\alpha$ -(1 $\rightarrow$ 2)-,  $\alpha$ -(1 $\rightarrow$ 3)-, and  $\alpha$ -(1 $\rightarrow$ 6)-Linked Mannosyl Disaccharides with MM3(92)', *Journal of Carbohydrate Chemistry*, 14: 4, 589 – 600

**To link to this Article:** DOI: 10.1080/07328309508005360

**URL:** <http://dx.doi.org/10.1080/07328309508005360>

PLEASE SCROLL DOWN FOR ARTICLE

Full terms and conditions of use: <http://www.informaworld.com/terms-and-conditions-of-access.pdf>

This article may be used for research, teaching and private study purposes. Any substantial or systematic reproduction, re-distribution, re-selling, loan or sub-licensing, systematic supply or distribution in any form to anyone is expressly forbidden.

The publisher does not give any warranty express or implied or make any representation that the contents will be complete or accurate or up to date. The accuracy of any instructions, formulae and drug doses should be independently verified with primary sources. The publisher shall not be liable for any loss, actions, claims, proceedings, demand or costs or damages whatsoever or howsoever caused arising directly or indirectly in connection with or arising out of the use of this material.

**MOLECULAR MECHANICS MODELING OF  $\alpha$ -(1 $\rightarrow$ 2)-,  $\alpha$ -(1 $\rightarrow$ 3)-, AND  
 $\alpha$ -(1 $\rightarrow$ 6)-LINKED MANNOSYL DISACCHARIDES WITH MM3(92)<sup>1</sup>**

Michael K. Dowd,\* Alfred D. French

Southern Regional Research Center  
U. S. Department of Agriculture, New Orleans, LA 70179

and Peter J. Reilly

Department of Chemical Engineering  
Iowa State University, Ames, IA 50011

*Received September 27, 1994 - Final Form December 21, 1994*

**ABSTRACT**

MM3(92) was used to study the conformational flexibility of  $\alpha$ -(1 $\rightarrow$ 2),  $\alpha$ -(1 $\rightarrow$ 3), and  $\alpha$ -(1 $\rightarrow$ 6)-linked mannosyl dimers. Mannosyl rings were allowed to relax, and several sets of *exo*-cyclic orientations were included in the study. Two- and three-dimensional Ramachandran energy representations are similar to those for glucosyl dimers with related linkages. Crystal structures lie in low-energy regions of the maps near local minima. Our results are compared with those presented earlier based on other modeling methods.

**INTRODUCTION**

Understanding glycoprotein conformation is important because of the key role these compounds play in biological recognition processes. The carbohydrate moieties are either *O*-linked to the protein through a serine or threonine side-chain or *N*-linked through an asparagine residue. Although several monosaccharides are found in these oligomers, mannosyl residues are especially common. For example, the core of *N*-linked oligosaccharides consists of a 3,6-di-*O*-( $\alpha$ -D-Man)-D-Man segment  $\beta$ -(1 $\rightarrow$ 4)-linked to

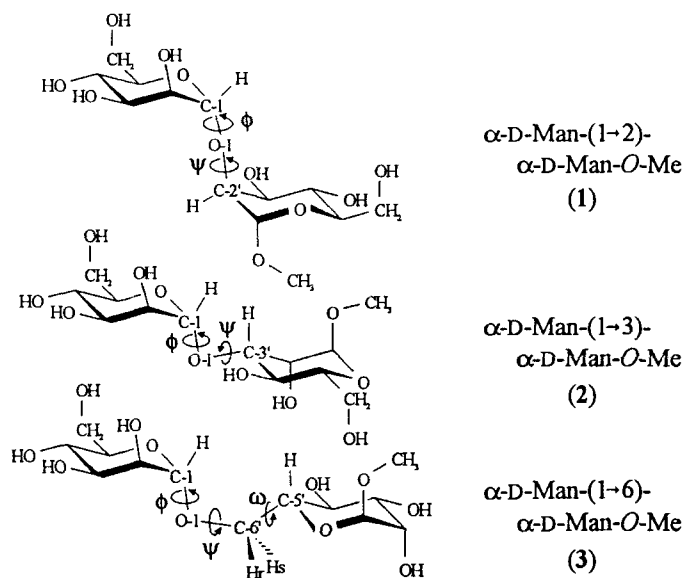


**Figure 1.** Molecular structures for  $\alpha$ -D-Man-(1 $\rightarrow$ 2)- $\alpha$ -D-Man-O-Me (1),  $\alpha$ -D-Man-(1 $\rightarrow$ 3)- $\alpha$ -D-Man-O-Me (2), and  $\alpha$ -D-Man-(1 $\rightarrow$ 6)- $\alpha$ -D-Man-O-Me (3).

the non-reducing residue of chitobiose. Several additional  $\alpha$ -(1 $\rightarrow$ 2)-,  $\alpha$ -(1 $\rightarrow$ 3)-, or  $\alpha$ -(1 $\rightarrow$ 6)-linked mannosyl residues are generally attached to this core.

We have already modeled several disaccharides, including the  $\alpha$ -(1 $\rightarrow$ 2)-,  $\alpha$ -(1 $\rightarrow$ 3)- and  $\alpha$ -(1 $\rightarrow$ 6)-linked glucosyl dimers, with the molecular mechanics program MM3.<sup>2-5</sup> The results predicted crystalline conformations well and have helped to develop a qualitative picture of the solution state. In this work, we apply our strategy that combines relaxed-residue modeling with multiple sets of starting conformers to the investigation of the structure of common mannosyl dimer fragments found within glycoprotein oligosaccharides. The structures modeled are shown in Figure 1.

## COMPUTATIONAL METHODS

A brief description of the computational methods will be presented here, as detailed descriptions have appeared earlier.<sup>2,3,5</sup> The 1992 version of the molecular mechanics program MM3 was used.<sup>6</sup> Optimizations were performed with a dielectric constant ( $\epsilon$ ) of 4.0, as median values were found best to model condensed-phase systems of carbohydrates<sup>7</sup> as well as peptides and proteins.<sup>8</sup>

Starting structures were generated and pre-optimized with PC-Model (Serena Software, Bloomington, IN). For each molecule, several sets of *exo*-cyclic orientations were included. *Gauche-gauche* (*gg*) ( $\text{H}(\text{C}-5)-\text{C}-5-\text{C}-6-\text{O}-6 = 180^\circ$ ) and *gauche-trans* (*gt*) ( $\text{H}(\text{C}-5)-\text{C}-5-\text{C}-6-\text{O}-6 = -60^\circ$ ) orientations were considered for the hydroxymethyl groups of both rings as were the closest approximations of clockwise and reverse-clockwise orientations of the secondary hydroxyl groups. The methoxy group at C-1' was placed in the orientation favored by the *exo*-anomeric effect ( $60^\circ$  to O-5'). Because the linkage of the  $\alpha$ -(1 $\rightarrow$ 3) dimer interferes with the formation of a hydrogen-bonding crown around the ring at the reducing end, several additional orientations of the secondary hydroxyl groups at C-2' and C-4' were included. In total, 16 sets of *exo*-cyclic orientations were considered for the  $\alpha$ -(1 $\rightarrow$ 2)-linked dimer, 32 sets for the  $\alpha$ -(1 $\rightarrow$ 3)-linked dimer, and eight sets for the  $\alpha$ -(1 $\rightarrow$ 6)-linked dimer.

The linkage torsion angles are defined as  $\phi = \text{H}(\text{C}-1)-\text{C}-1-\text{O}-1-\text{C}-i$ , where  $i = 2', 3',$  or  $6'$  depending on the disaccharide;  $\psi = \text{C}-1-\text{O}-1-\text{C}-i-\text{H}(\text{C}-i)$ , where  $i = 2'$  or  $3'$  for the  $\alpha$ -(1 $\rightarrow$ 2) and  $\alpha$ -(1 $\rightarrow$ 3) dimers, and  $\psi = \text{C}-1-\text{O}-1-\text{C}-6'-\text{C}-5'$  and  $\omega = \text{O}-1-\text{C}-6'-\text{C}-5'-\text{H}(\text{C}-5')$  for the  $\alpha$ -(1 $\rightarrow$ 6) dimer. Conformational space about the glycosidic torsion angles was studied in  $20^\circ$  increments, and all other geometric features were allowed to optimize. The block-diagonal optimization method with the default termination criterion was used for grid-point energy minimizations. At each grid position, the lowest-energy structure from the populations of starting conformations was used to construct a conformational map. Contoured maps were generated with Surfer (Golden Software, Golden, CO). For the  $\alpha$ -(1 $\rightarrow$ 6)-linked dimer, rendered iso-energy surfaces were constructed with Dicer (Spyglass, Inc., Savoy, IL). For the two-bond-linked disaccharides, these maps are expressed with  $\phi$  and  $\psi$  values ranging from  $-180^\circ$  to  $180^\circ$ . For the  $\alpha$ -(1 $\rightarrow$ 6)-linked structure, the  $\phi$ - $\psi$ - $\omega$  volume and  $\phi$ - $\psi$  contour plots are expressed with  $\phi$  ranging from  $-180^\circ$  to  $180^\circ$  and with  $\psi$  and  $\omega$  ranging from  $0^\circ$  to  $360^\circ$ . These representations were chosen to keep contours or surfaces from being drawn on plot edges.

Local minima were derived from the indicated low-energy regions of the maps. These minima were generated from grid-point optimized local structures by releasing the torsion angle constraints. Every starting conformer that appeared within the local region ( $\pm 20^\circ$ ) that contributed to the adiabatic map or surface was considered in determining the local minima. These final optimizations used the MM3 full-matrix method. Boltzmann-weighted three-bond hydrogen-hydrogen and carbon-hydrogen coupling constants were estimated from the Karplus-type equations of Haasnoot et al.<sup>9</sup> and Tvaroška et al.,<sup>10</sup> respectively. The complete adiabatic surfaces were used for these estimations.

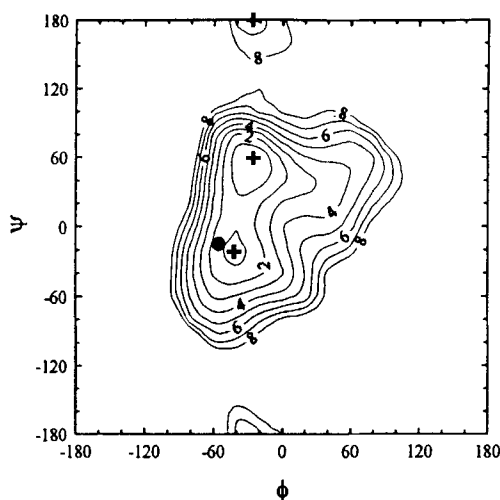


**Figure 2.** MM3(92) ( $\epsilon = 4.0$ )  $\phi$ - $\psi$  conformational map for  $\alpha$ -D-Man-(1 $\rightarrow$ 2)- $\alpha$ -D-Man-O-Me (**1**). Crosses (+) represent local MM3 minima. The filled circle (●) represents the published crystal structure of Srikrishnan et al.<sup>11</sup>

## RESULTS

The  $\phi$ - $\psi$  map for **1** is given in Figure 2. Three low-energy regions are found on this surface. All three have  $\phi$  values that are in accord with the *exo*-anomeric effect. Two of these regions are similar in energy and are likely to be important in understanding solution conformation. The third is quite high in energy and is unlikely to be significant. Also shown is the position of the x-ray crystallographic structure of **1** determined by Srikrishnan et al.<sup>11</sup> The linkage conformations of the structures at local minima plus their energies are given in Table 1.

The  $\phi$ - $\psi$  map for **2** is given in Figure 3. This map exhibits four minima within 8 kcal/mol, although two of these are relatively high in energy. The figure also denotes the  $\phi$ - $\psi$  orientation of the Man- $\alpha$ -(1 $\rightarrow$ 3)-Man moiety from a single crystal study of  $\alpha$ -D-Man-(1 $\rightarrow$ 3)- $\beta$ -D-Man-(1 $\rightarrow$ 4)-GlcNAc by Warin et al.<sup>12</sup> Table 1 contains the glycosidic orientations and energies of the locally-derived minima.

Adiabatic iso-energy surfaces within the  $\phi$ - $\psi$ - $\omega$  conformational space of **3** are presented in Figure 4. These surfaces are shown at 2, 4, 6, and 8 kcal/mol above the global minimum. Contour surfaces at eclipsed and staggered  $\omega$  orientations are shown in Figure 5. Nine individual low-energy regions are found within 8 kcal/mol of the global minimum. The nine local minima are described in Table 1.

**Table 1.** Local minima for the  $\alpha$ -(1 $\rightarrow$ 2)-,  $\alpha$ -(1 $\rightarrow$ 3)-, and  $\alpha$ -(1 $\rightarrow$ 6)-linked mannosyl disaccharides from MM3(92) at  $\epsilon = 4.0$ .

Disaccharide	$\phi$ (degrees)	$\psi$ (degrees)	$\omega$ (degrees)	MM3(92) Energy (kcal/mol)	Relative Energy (kcal/mol)
$\alpha$ -D-Man-(1 $\rightarrow$ 2)-					
$\alpha$ -D-Man- <i>O</i> -Me (1)	-25.5	60.1	-	26.07	0
	-42.4	-21.3	-	26.79	0.72
	-26.6	179.9	-	32.05	5.98
$\alpha$ -D-Man-(1 $\rightarrow$ 3)-					
$\alpha$ -D-Man- <i>O</i> -Me (2)	-20.5	49.9	-	24.89	0
	-44.7	-11.7	-	24.94	0.05
	-29.6	-159.8	-	28.76	3.87
	168.3	17.0	-	32.48	7.59
$\alpha$ -D-Man-(1 $\rightarrow$ 6)-					
$\alpha$ -D-Man- <i>O</i> -Me (3)	-41.4	188.0	177.3	22.60	0
	-45.0	186.8	309.0	23.02	0.42
	-44.7	186.4	60.8	23.22	0.62
	-43.3	82.7	305.3	24.75	2.15
	-44.2	87.8	162.6	25.06	2.46
	-28.0	298.4	331.4	25.69	3.09
	3.4	287.0	51.7	26.63	4.03
	-12.3	285.1	198.5	28.02	5.42
	155.1	175.4	58.7	30.58	7.98

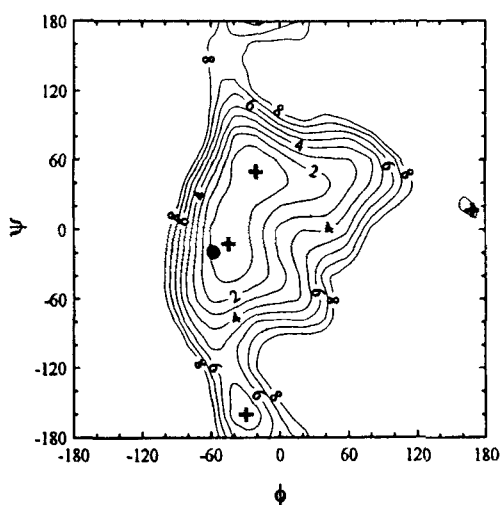


**Figure 3.** MM3(92) ( $\epsilon = 4.0$ )  $\phi$ - $\psi$  conformational map for  $\alpha$ -D-Man-(1 $\rightarrow$ 3)- $\alpha$ -D-Man-*O*-Me (2). Crosses (+) represent local MM3 minima. The filled circle (●) represents the published crystal structure of Warin et al.<sup>12</sup>

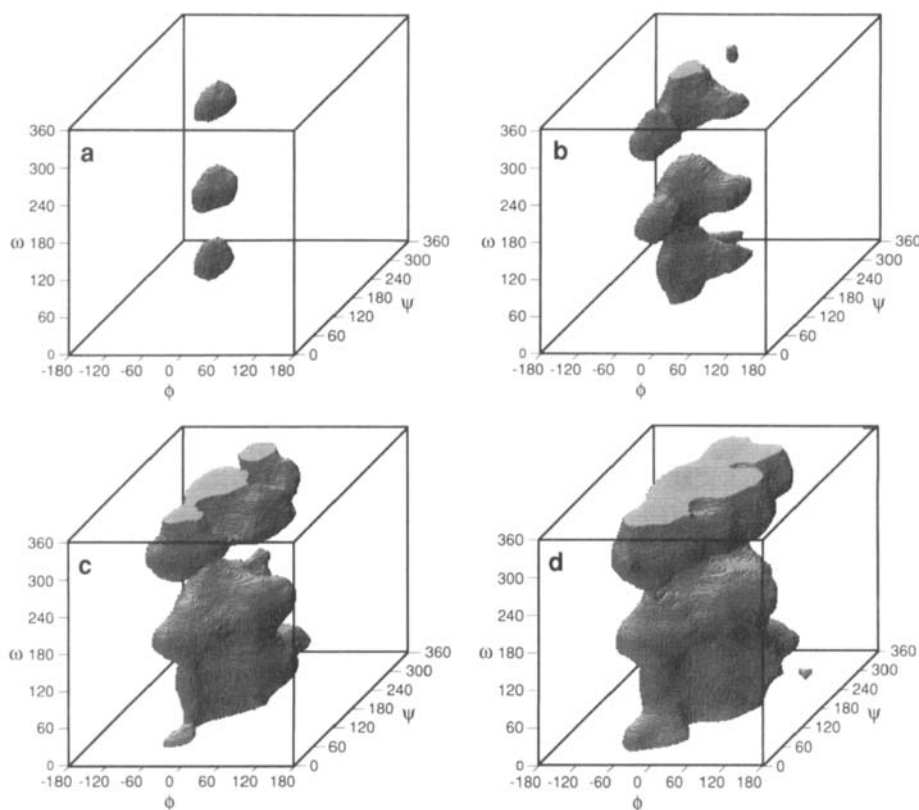


**Figure 4.** MM3(92) ( $\epsilon = 4.0$ )  $\phi$ - $\psi$ - $\omega$  conformational volumes for  $\alpha$ -D-Man-(1 $\rightarrow$ 6)- $\alpha$ -D-Man-O-Me. Iso-energy surfaces are shown at 2 kcal/mol (a), 4 kcal/mol (b), 6 kcal/mol (c), and 8 kcal/mol (d).

For the  $\alpha$ -(1 $\rightarrow$ 2)-linked dimer, glycosidic coupling constants for  $J_{\text{H}(\text{C}-1)-\text{C}-2'}$  of 4.0 Hz and  $J_{\text{C}-1-\text{H}(\text{C}-2')}$  of 3.0 Hz are calculated by conformational averaging over the adiabatic surface. For the  $\alpha$ -(1 $\rightarrow$ 3)-linked dimer,  $J_{\text{H}(\text{C}-1)-\text{C}-3'}$  = 3.9 Hz and  $J_{\text{C}-1-\text{H}(\text{C}-3')}$  = 3.8 Hz. For the  $\alpha$ -(1 $\rightarrow$ 6)-linked disaccharide,  $J_{\text{H}(\text{C}-1)-\text{C}-6'}$  = 3.2 Hz,  $J_{\text{C}-1-\text{Hs}(\text{C}-6')}$  = 1.6 Hz,  $J_{\text{C}-1-\text{Hr}(\text{C}-6')}$  = 2.3 Hz,  $J_{\text{H}(\text{C}-5')-\text{Hs}(\text{C}-6')}$  = 4.4 Hz, and  $J_{\text{H}(\text{C}-5')-\text{Hr}(\text{C}-6')}$  = 4.8 Hz.

We have previously calculated a molecular partition function,  $q = \sum \exp(-E_i/RT)$ , as an indication of the flexibility about the glycosidic linkages. As a general trend based on the glucosyl disaccharides we found that three-bond-linked molecules, with  $q$  values ranging from 8 to 14 (based on a 20° grid spacing and a single energy value at each grid-point), have more flexibility than two-bond linked disaccharides, with corresponding values ranging from 2 to 8.<sup>2,3,5</sup> A similar ordering is obtained for the three mannosyl

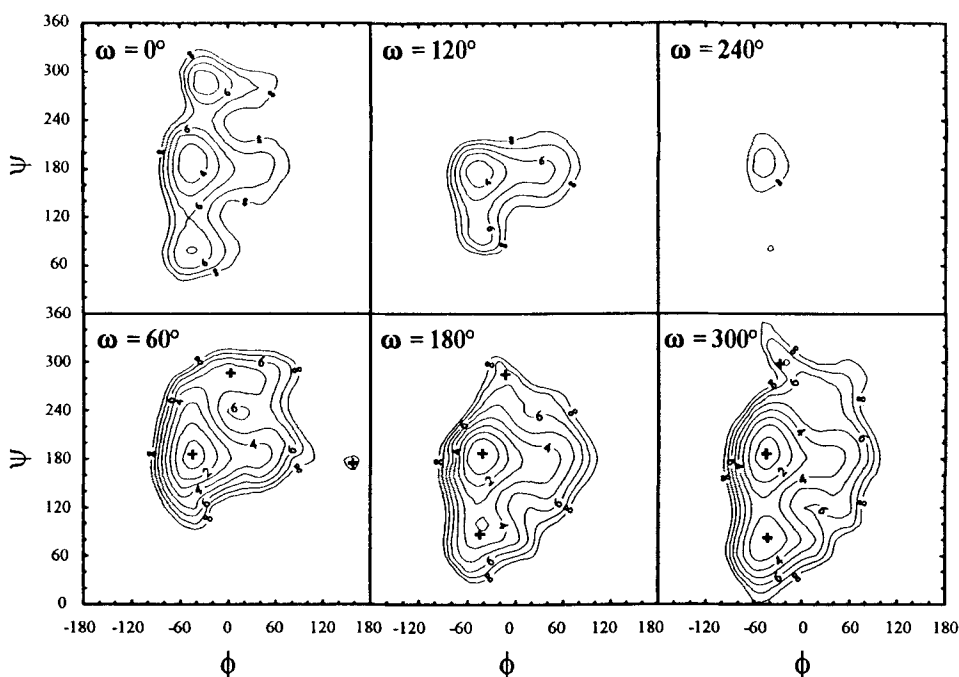


**Figure 5.** MM3(92) ( $\epsilon = 4.0$ )  $\phi$ - $\psi$  contour maps for  $\alpha$ -D-Man-(1 $\rightarrow$ 6)- $\alpha$ -D-Man-O-Me with eclipsed and staggered orientations of the  $\omega$  torsion angle. Crosses (+) represent the projected locations of local minima. Local minima differ by up to  $29^\circ$  from the  $\omega$  orientations represented (see Table 1).

dimers studied here, which have  $q$  values for the  $\alpha$ -(1 $\rightarrow$ 6),  $\alpha$ -(1 $\rightarrow$ 3), and  $\alpha$ -(1 $\rightarrow$ 2)-linked dimers of 8.1, 6.8, and 3.4, respectively.

## DISCUSSION

**$\alpha$ -D-Man-(1 $\rightarrow$ 2)- $\alpha$ -D-Man-O-Me (1).** Several computational methods have been used to study this disaccharide and oligomers containing this moiety. Early work focused on searching for local minima,<sup>13,14</sup> with later reports describing conformational  $\phi$ - $\psi$  maps based on rigid-residue methodology or molecular dynamics.<sup>15-20</sup> Computational techniques have included a potential function accounting for nonbonded, electrostatic, and torsional effects,<sup>13</sup> HSEA and variants,<sup>14,19,20</sup> MNDO,<sup>16</sup> modified versions of AMBER,<sup>16,17</sup> and PFOS.<sup>18</sup> From these methods three low-energy conformational regions were repeatedly found by at least two of the methods. These include ( $\pm 25^\circ$ ) the  $\phi \sim -40^\circ$ ,  $\psi \sim -40^\circ$  region (A), the  $\phi \sim -40^\circ$ ,  $\psi \sim 40^\circ$  region (B), and the  $\phi \sim 40^\circ$ ,  $\psi \sim 40^\circ$  region (C).

No relaxed-residue map for this disaccharide has previously been presented. As it has for other disaccharides, the relaxed-residue approach has allowed the accessible conformational space to expand. The map is similar to the MM3(90) map of leucrose,<sup>4</sup> which also has an axial-axial glycosidic linkage. The two lowest-energy regions correspond with the **A** and **B** regions as given above. The **C** region does not exist as a minimum on the MM3 map although relatively low-energy contours (<4 kcal/mol) extend in this direction.

In general, we have found that conformations of crystalline disaccharides lie within 2 to at most 3 kcal/mol of the global minima on MM3  $\phi$ - $\psi$  maps. A crystal structure has been reported for **1** with the glycosidic torsion angles of  $\phi = -55.5^\circ$  and  $\psi = -14.5^\circ$ .<sup>11</sup> This structure is located within 1.5 kcal/mol of the global minimum and is very close to the MM3 second lowest-energy minimum (Figure 2).

Substantial effort has been applied to the understanding of mannosyl oligomers in solution. Much of this work has centered on interpreting NOE measurements. Early reports focused on identifying a single conformational region that would reproduce the experimental data. With the realization that conformational averaging of a population of conformers represented a more realistic model of solution behavior, computational reports began to focus on Boltzmann-weighted averaging of modeled surfaces for predicting NOE values. Peters<sup>19</sup> reported that conformational averaging of the HSEA-based surface yielded better agreement between modeled and measured NOEs and <sup>1</sup>H NMR relaxation times than for modeled values based on the global minimum. This result implies that some molecules from the **B** region contribute to the population. A similar conclusion was reported by Helander et al.<sup>20</sup> Stevens<sup>21</sup> has also studied the solution structure with a conformation-dependent model of optical rotation. He showed that the **A** region yielded the observed optical rotation, the **B** region had optical rotation higher than observed, and the **C** region had values lower than observed. Therefore significant excursions into the **B** region must be compensated for by excursions into the **C** region. Within the accuracy of his model, it is possible that ~20% of the population could exist within the **B** region without a significant contribution from **C**. Taken together, it appears that the solution structure includes a large and possibly dominant population with the **A** region conformation with some contribution from the **B** region and possibly a minor contribution from the third region. Our MM3 map yields minima in the two important regions, although the relative order of steric energies is opposite to that suggested above. Part of this discrepancy may be due to an intramolecular hydrogen bond that occurs between the O-6 and H(O-6') atoms in the global low-energy region of our map that stabilizes this conformational region in vacuum but would not be important in aqueous solution. In addition, specific solvation effects and entropic differences have

not been taken into account in the model and may also contribute to the deviations. The possibility of modeling error of the order of  $\sim 1$  kcal/mol cannot be overlooked either.

**$\alpha$ -D-Man-(1 $\rightarrow$ 3)- $\alpha$ -D-Man-O-Me (2).** Conformational searches, steric contact maps, rigid-residue maps, and relaxed-residue maps have been presented for the  $\alpha$ -(1 $\rightarrow$ 3)-linked moiety. Conformational searches and rigid-residue maps have been described based on the same potential function accounting for nonbonded, electrostatic, and torsional effects mentioned above,<sup>13,22</sup> as well as with HSEA,<sup>23-25</sup> MNDO,<sup>16</sup> PFOS,<sup>18</sup> and PIM.<sup>26</sup> The two low-energy regions ( $\pm 25^\circ$ ) identified by most of the methods are  $\phi \sim -40^\circ$ ,  $\psi \sim -40^\circ$  (**A**) and  $\phi \sim -40^\circ$ ,  $\psi \sim 40^\circ$  (**B**). A third region near  $\phi \sim 40^\circ$ ,  $\psi \sim 40^\circ$  (**C**) is identified with the simple nonbonded, electrostatic, and torsional potential as well as by PFOS and PIM with energies between  $\sim 1.5$  and 3 kcal/mol above the global minimum. Other minima have been identified, particularly with PFOS and PIM, but generally these have energies greater than 4 kcal/mol above the global minimum. Relaxed-residue maps have been published for this structure with earlier original and modified versions of Allinger's software. Both of these maps yield low-energy regions corresponding to the **A** and **B** regions above. An MM2(85) map of the  $\beta$ -anomeric form of this methyl mannoside is similar to Figure 3 except for a shallow minimum on the older map corresponding to the **C** region that is  $>3$  kcal/mol above the global minimum.<sup>27</sup> Additional minima were reported from a relaxed MM2CARB map.<sup>28</sup> These MM2CARB minima are assumed to result from the inclusion of *trans-gauche* hydroxymethyl orientations that we normally do not include, as they are not thought to be important in solution (MM2 and MM3 will favor the *trans-gauche* orientation in calculations with low dielectric constants). The MM3(92) map presented here is also similar to the MM3(90) map of nigerose,<sup>2</sup> the  $\alpha$ -(1 $\rightarrow$ 3) dimer of glucose. Both structures are axially-equatorially linked.

A crystal structure of  $\alpha$ -D-Man-(1 $\rightarrow$ 3)- $\alpha$ -D-Man-(1 $\rightarrow$ 4)- $\alpha$ -D-GlcNAc has  $\phi$  and  $\psi$  values of  $-57.6^\circ$  and  $-19.4^\circ$ , respectively.<sup>12</sup> This orientation lies within the 1 kcal/mol contour line of the MM3(92) map.

In early work, two groups have attempted to explain experimental NOEs in terms of a single conformational region. Brisson and Carver<sup>23</sup> proposed an **A** conformation, while Homans and co-workers<sup>15</sup> proposed the **B** region. More recently, Boltzmann-weighted averaging of a population of conformations has been used to estimate NOE values. Experimental evidence suggesting internal motion for this disaccharide has recently been reported.<sup>29</sup> Not surprisingly, results from conformational averaging depend on the methods used for generating individual energies or probabilities.<sup>27</sup> Stevens has shown for the  $\alpha$ -(1 $\rightarrow$ 3) dimer that the **B** region yields the correct optical rotation and that a large population within the **A** region, which has high optical rotation

values, must be compensated for by a population in the C region, with low values of the optical rotation.<sup>30</sup> Yet within the expected accuracy of this approach, a 70:30 ratio of the first two conformational regions is possible without a significant contribution from the third. This corresponds to an energy difference of  $\sim 0.4$  kcal/mol. From the MM3(92) map, the A and B regions are equally probable. No important intra-residue hydrogen bonds to skew the vacuum-based populations were identified. As both regions have now been identified with a variety of computational methods and internal motion exists for this disaccharide, some combination of these two conformational regions is likely.

**$\alpha$ -D-Man-(1 $\rightarrow$ 6)- $\alpha$ -D-Man-O-Me (3).** This disaccharide has been modeled with HSEA<sup>23,31</sup> MNDO,<sup>16</sup> modified AMBER,<sup>17</sup> PFOS<sup>18</sup> and PIM.<sup>26</sup> Rigid-residue  $\phi$ - $\psi$  maps have been generated at fixed  $\omega$  orientations of  $180^\circ$  and  $-60^\circ$  with HSEA, MNDO, PFOS and PIM. (The  $\omega = 60^\circ$  orientation is generally neglected as it is thought to be less significant.) The HSEA, PFOS, and PIM methods identified low-energy minima near  $\phi \sim -40^\circ$ ,  $\psi \sim 180^\circ$ , and with  $\omega \sim 180^\circ$  (A) or  $-60^\circ$  (B). MNDO identifies a wide range of  $\psi$ , including  $\psi \sim 180^\circ$ . Relaxed-residue maps have not been reported for this disaccharide. The MM3(92) relaxed-residue three-dimensional  $\phi$ - $\psi$ - $\omega$  surfaces presented here are quite similar to those for  $\alpha$ -isomaltose, the related  $\alpha$ -(1 $\rightarrow$ 6)-linked glucosyl disaccharide.<sup>5</sup> Within 8 kcal/mol of the global minimum, nine minima regions exist, although many are relatively high in energy and are unlikely to be significant. As with many of the methods mentioned above, the  $\phi \sim -40^\circ$  and  $\psi \sim 180^\circ$  regions are the lowest in energy. Of the staggered  $\omega$  torsion angles, the most favored is the  $180^\circ$  orientation (A) followed by the  $-60^\circ$  (B), and the least favored is the  $60^\circ$  orientation. However, the MM3-calculated difference between the  $\omega = 60^\circ$  and  $-60^\circ$  wells is much smaller for the mannosyl dimer than it was for isomaltose.

Hydrogen-hydrogen coupling constants characteristic of the torsion angle about the C-5'-C-6' bond have been reported for several mannosyl oligomers containing  $\alpha$ -(1 $\rightarrow$ 6) linkages.<sup>31-33</sup> Cummings and Carver gave coupling constants for **3** of  $J_{\text{H}(\text{C-5}')-\text{H}_s(\text{C-6}')} = 1.8$  Hz and  $J_{\text{H}(\text{C-5}')-\text{H}_r(\text{C-6}')} = 6.1$  Hz.<sup>31</sup> Variation in the experimental values for higher mannosyl oligomers indicates that the distribution of rotamers is affected by the primary sequence of the oligomer ( $J_{\text{H}(\text{C-5}')-\text{H}_r(\text{C-6}')}$  values from  $3.4 \pm 0.5$  to  $5.5 \pm 0.5$  Hz).<sup>33</sup> These values suggest that a mixture of  $\omega = 180^\circ$  and  $-60^\circ$  rotamers exists. The calculated value for  $J_{\text{H}(\text{C-5}')-\text{H}_s(\text{C-6}')}$  of 4.4 Hz compared to the experimental values of 1.8 to 2.2 Hz indicates that the  $\omega = 60^\circ$  orientation, which has an MM3 energy only 0.62 kcal/mol above the global minimum, is overemphasized in the conformational average. Part of this discrepancy may be attributable to the stabilizing influence of an intramolecular hydrogen bond in the  $\omega = 60^\circ$  region between the O-1 and H(O-4') atoms

within the vacuum model, although we note that this hydrogen-bond also occurred for isomaltose yet did not skew the conformational equilibrium as severely. Brisson and Carver<sup>23</sup> have also reported carbon-hydrogen coupling constants for methyl manno-trioside across the O-1-C-6' bond of  $J_{C-1-Hs(C-6')} = 1.0 \pm 0.5$  Hz and  $J_{C-1-Hr(C-6')} = 2.5 \pm 0.1$  Hz, which indicates that a *trans* orientation of the two rings is dominant ( $\psi \sim 180^\circ$ ). These values are in good agreement with the modeled values given above.

## CONCLUSIONS

Relaxed-residue conformational maps have been presented for the  $\alpha$ -(1 $\rightarrow$ 2)-,  $\alpha$ -(1 $\rightarrow$ 3)-, and  $\alpha$ -(1 $\rightarrow$ 6)-linked disaccharides of mannose based on the molecular mechanics program MM3(92). The maps are similar to those previously published for glucosyl and glucosyl-fructosyl disaccharides with similar glycosidic linkages. Single crystal structures containing these dimer moieties lie in low-energy wells of the MM3 surfaces within 1.5 kcal/mol of the MM3(92) global minimum. While the results are consistent with current understanding of solution structure, small inaccuracies of the model prevented the development of an improved picture of the conformational behavior of these compounds in solution.

## REFERENCES AND NOTES

1. This work was presented at the *XVII International Carbohydrate Symposium*, Ottawa, Canada, July 17-22, 1994.
2. M. K. Dowd, J. Zeng, A. D. French and P. J. Reilly, *Carbohydr. Res.*, **230**, 223 (1992).
3. M. K. Dowd, A. D. French and P. J. Reilly, *Carbohydr. Res.*, **233**, 15 (1992).
4. M. K. Dowd, P. J. Reilly and A. D. French, *J. Carbohydr. Chem.*, **12**, 449 (1993).
5. M. K. Dowd, P. J. Reilly and A. D. French, *Biopolymers*, **34**, 625 (1994).
6. N. L. Allinger, Y. H. Yuh and J. H. Lii, *J. Am. Chem. Soc.*, **111**, 8551 (1989); J. H. Lii and N. L. Allinger, *J. Am. Chem. Soc.*, **111**, 8566 (1989); N. L. Allinger, M. Rahman and J. H. Lii, *J. Am. Chem. Soc.*, **112**, 8293 (1990).
7. A. D. French and M. K. Dowd, *J. Mol. Struct. (Theochem)*, **286**, 183 (1993).
8. J.-H. Lii and N. L. Allinger, *J. Comput. Chem.*, **12**, 186 (1991).
9. C. A. G. Haasnoot, F. A. A. M. de Leeuw and C. Altona, *Tetrahedron*, **36**, 2783 (1980).
10. I. Tvaroška, M. Hricovíni and E. Petráková, *Carbohydr. Res.*, **189**, 359 (1989).
11. T. Srikrishnan, M. S. Chowdhary and K. L. Matta, *Carbohydr. Res.*, **186**, 167 (1989).
12. V. Warin, F. Baert, R. Fouret, G. Strecker, G. Spik, B. Fournet and J. Montreuil, *Carbohydr. Res.*, **76**, 11 (1979).

13. M. Biswas and V. S. R. Rao, *Int. J. Quantum Chem.*, **20**, 99 (1981).
14. J.-R. Brisson and J. P. Carver, *Biochemistry*, **22**, 3671 (1983).
15. S. W. Homans, A. Pastore, R. A. Dwek and T. W. Rademacher, *Biochemistry*, **26**, 6649 (1987).
16. S. W. Homans, C. J. Edge, M. A. J. Ferguson, R. A. Dwek and T. W. Rademacher, *Biochemistry*, **28**, 2881 (1989).
17. C. J. Edge, U. C. Singh, R. Bazzo, G. L. Taylor, R. A. Dwek and T. W. Rademacher, *Biochemistry*, **29**, 1971 (1990).
18. A. Imberty, S. Gerber, V. Tran and S. Pérez, *Glycoconjugate J.*, **7**, 27 (1990).
19. T. Peters, *Liebigs Ann. Chem.*, 135 (1991).
20. A. Helander, L. Kenne, S. Oscarson, T. Peters and J.-R. Brisson, *Carbohydr. Res.*, **230**, 299 (1992).
21. E. S. Stevens, *Biopolymers*, **34**, 1403 (1994).
22. M. Biswas, Y. C. Sekharudu and V. S. R. Rao, *Int. J. Biol. Macromol.*, **8**, 2 (1986).
23. J.-R. Brisson and J. P. Carver, *Biochemistry*, **22**, 1362 (1983).
24. H. Paulsen, T. Peters, V. Sinnwell, R. Lebuhn and B. Meyer, *Liebigs Ann. Chem.*, 951 (1984).
25. J. P. Carver, S. W. Michnick, A. Imberty and D. A. Cumming, in *Carbohydrate Recognition in Cellular Function*, Ciba Foundation Symposium 145, New York, 1989, pp 6-26.
26. A. Imberty, S. Pérez, M. Hricovini, R. N. Shah and J. P. Carver, *Int. J. Biol. Macromol.*, **15**, 17 (1993).
27. J. P. Carver, D. Mandel, S. W. Michnick, A. Imberty and J. W. Brady, *ACS Symp. Ser.*, **430**, 266 (1990).
28. A. Imberty, V. Tran and S. Pérez, *J. Comput. Chem.*, **11**, 205 (1989).
29. M. Hricovini, R. N. Shah and J. P. Carver, *Biochemistry*, **31**, 10018 (1992).
30. E. S. Stevens, *Biopolymers*, **34**, 1395 (1994).
31. D. A. Cummings and J. P. Carver, *Biochemistry*, **26**, 6676 (1987).
32. F. M. Winnik, J.-R. Brisson, J. P. Carver and J. J. Krepinsky, *Carbohydr. Res.*, **103**, 15 (1982).
33. E. W. Wooten, R. Basso, C. J. Edge, S. Zamze, R. A. Dwek and T. W. Rademacher, *Eur. Biophys. J.*, **18**, 139 (1990).